

Neutron Anomalous-Moment Contributions to Muonic Isomer Shifts in ^{207}Pb R. Anigstein, B. Budick, and J. W. Kast^(a)*Physics Department, New York University, New York, New York 10003*
(Received 20 March 1980)

The muonic isomer shifts of three transitions between levels of ^{207}Pb have been measured. Evidence is found for an interaction between the anomalous magnetic moment of the neutron hole and the electric field of the $1s$ muon. The agreement obtained between predicted and measured values removes the necessity to postulate a more serious reaction in the proton core to changes in the state of the valence neutron than predicted by the weak coupling model.

PACS numbers: 21.10Pc, 36.10Gv

When a nucleus deexcites radiatively in the presence of a muon in the $1s$ level there is generally a shift in the energy of the nuclear γ ray from its normal value. Such shifts, referred to as muonic isomer shifts, are usually attributed to differences in the nuclear charge distribution in the ground and excited states which produce corresponding differences in the muon's binding energy. Observation of muonic isomer shifts is made possible by nuclear excitation during the atomic cascade of the muon. At some stage the muon undergoes a radiationless transition and proceeds to the $1s$ level in roughly 10^{-17} sec. There is usually ample time for the nucleus to deexcite before the muon is captured by the nucleus (10^{-7} sec).

Although the hyperfine structure due to the $1s$ muon does not shift the center of gravity of a level it may lead to an apparent shift in the nuclear γ ray. The populations of the excited hyperfine levels may not be statistical because of some selection rule in the excitation process. In addition, a fast $M1$ Auger transition can occur between the hyperfine levels of the excited state which depopulates the upper level. A shift in the centroid of an unresolved hyperfine multiplet will result.

Nuclear polarization by the $1s$ muon contributes to the isomer shift only in second-order perturbation theory. In this order the effects are mainly due to virtual excitations to highly collective states. If ground and excited nuclear states differ only in the *spin* of a valence nucleon, the *difference* in the nuclear polarization in these states should be small and contribute little to the isomer shift.

We report here the first evidence for a new contribution to the isomer shift, and to muonic energy levels in general. For heavy nuclei the $1s$ muon spends roughly 50% of its time within the orbital radius of the valence nucleons. Consider the low-lying energy levels of ^{207}Pb shown in Fig. 1 which are fairly pure neutron hole states.² The

interaction of the anomalous magnetic moment of the neutron with the electric field of the muon is given by³

$$g(\mu_N/2Mc)\langle U_A^* | -\nabla \cdot \vec{E} + 2i\vec{\sigma} \cdot \vec{E} \times \nabla | U_A \rangle. \quad (1)$$

In this matrix element g is the anomalous moment factor (-1.91), μ_N is the nuclear magneton, M is the neutron mass, E is the electric field of the muon, and U_A are the large components of the neutron spinor.

The first term is the Foldy term,⁴ while the second can be understood classically as the interaction of the neutron magnetic moment with the magnetic field it sees by virtue of its motion through the muon's electric field. The second term can be transformed to its usual spin-orbit form by the substitutions

$$\vec{p} = -i\hbar\nabla, \quad \vec{s} = \frac{1}{2}\vec{\sigma},$$

$$\vec{E} = (\vec{r}_N/r_N^3)(-e)\int_0^{r_N}(f^2 + g^2)r^2 dr,$$

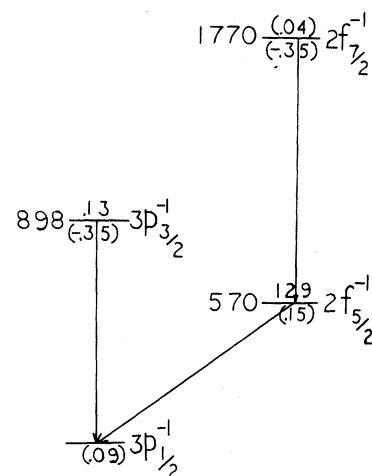


FIG. 1. Low-lying energy levels of ^{207}Pb . Lifetimes in picoseconds are given above each level (calculated value in parenthesis). Predicted hyperfine splitting constants are given below each level. (See Ref. 1.) Isomer shifts are reported for the indicated transitions.

where f and g are the Dirac radial functions for the muon in the nuclear potential. We find⁵

$$W = g\mu_N(e\hbar/Mc)2\vec{1} \cdot \vec{s} \int_0^\infty \psi_N^2(r_N) r_N^{-3} r_N^2 dr_N \int_0^{r_N} (f^2 + g^2) r^2 dr. \quad (2)$$

For a neutron *hole* the interaction increases the separation between the doublet p and f levels shown in Fig. 1. These interdoublet transitions are ideal for detecting the anomalous-moment contribution since they involve neutrons rather than protons, and involve no change in the orbital angular momentum of the neutron. Shifts in the energy of the nuclear γ ray due to differences in the charge distributions of ground and excited states, or due to differences in the nuclear polarization of these states should be minimal for such transitions. In addition, in our approximation [that simple oscillator functions suffice in the evaluation of the matrix element, Eq. (1)] the Foldy term makes no contribution to the interdoublet transition energy.

The interaction W occurs between the muon and each nucleon in the nucleus. The sum over nucleons with $j = l + \frac{1}{2}$ and $j = l - \frac{1}{2}$ vanishes identically. Moreover the sum over the twelve $h_{11/2}$ protons and the fourteen $i_{13/2}$ neutrons is small because of opposing contributions from neutrons and protons. Most important for our work, however, is that this sum is the same for both the excited state and the ground state and contributes nothing to the isomer shift.⁶

We note that the extraction of nuclear charge densities from high-energy electron scattering experiments requires that the interaction of the electron's field with the anomalous moments of both neutrons and protons be taken into account.⁷

Our experiment was performed in the muon channel of the Space Radiation Effects Laboratory (SREL) in Newport News, Virginia. A 164-gm lead target enriched to 92.8% in ^{207}Pb was viewed by both a 5-cm² × 1-cm planar intrinsic germanium detector and by a 35-cm³ coaxial lithium-drifted germanium detector. For the intrinsic detector our in-beam energy resolution at 898 keV was 1.34 keV full width at half maximum (FWHM), while our time resolution at this energy was 2.6 ns FWHM. The coaxial detector had an energy resolution of 4.07 keV at 1.77 MeV, and a time resolution of 19 ns FWHM.

Standard beam logic was employed and the SREL data acquisition system including an IBM 360/44 computer was used. For each event we recorded both the energy and time of arrival following the μ -stop signal. Calibration sources included ^{51}Cr , ^{131}I , ^{198}Au , ^{137}Cs , ^{88}Y , ^{22}Na , ^{60}Co , and ^{207}Bi , and were positioned as close as possible

to the target. Muonic and calibration spectra were accumulated simultaneously and with the same electronics.

Isomer shifts in the 570-keV and 1.770-MeV transitions were measured with respect to the normal γ rays in ^{207}Pb from the decay of ^{207}Bi . The energy of the normal $\frac{3}{2}^- \rightarrow \frac{1}{2}^-$ transition is known, 897.73 ± 0.09 keV. Its emission from ^{207}Bi is extremely weak. However, the ^{88}Y source has a γ ray at 898.045 ± 0.006 and provided an excellent reference in this region.

Our results for the $\frac{3}{2}^- \rightarrow \frac{1}{2}^-$ transition are shown in Fig. 2. We have succeeded in identifying several weak muonic x rays whose predicted yields are of the order of 0.01 per μ stop. By normalizing the intensity of the nuclear γ ray to the nearby $4f_{7/2} \rightarrow 3d_{5/2}$ transition (whose yield we have calculated as 0.40 per μ stop), we deduce a yield $0.7 \pm 0.2\%$ per μ stop for the former. This is lower than a previously reported value $1.2 \pm 0.3\%$.⁸ The peak at 905.5 keV appears in the spectrum of delayed events, while the peak at 901 keV may also

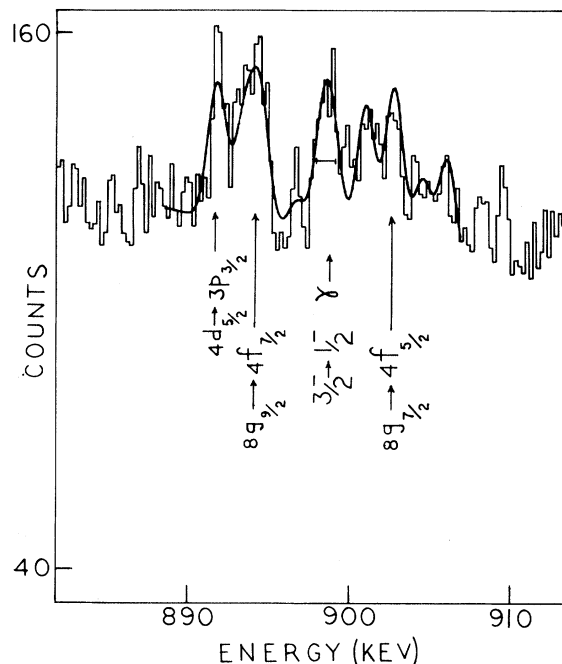


FIG. 2. Prompt spectrum in the vicinity of the $\frac{3}{2}^- \rightarrow \frac{1}{2}^-$ transition. Data taken with the planar intrinsic germanium detector. The horizontal error bar is the detector resolution FWHM. The smooth curve is the result of our computer analysis.

TABLE I. Predicted and measured isomer shifts in transitions between the low-lying levels of ^{207}Pb . All entries are in kiloelectronvolts. The entries in the final column include the hyperfine-structure corrections.

Transition	Energy ^a	$\Delta E_{\uparrow, \downarrow}^{\uparrow, \downarrow}$	ΔE_F^b	$\Delta E_{w.c.}^c$	ΔE_E^d	ΔE_{sum}	ΔE_{exp}
$3p_{3/2}-3p_{1/2}$	897.73	+0.51	+0.41	0.2-0.3	1.5 ± 0.5	0.76	0.74 ± 0.20
$2f_{7/2}-2f_{5/2}$	1770.2	+1.18	+0.44	1.0-1.4	6.3 ± 0.8	2.38	3.3 ± 0.6
$2f_{5/2}-3p_{1/2}$	569.704	-0.34	+0.67	0.1-0.2	0.1 ± 0.5	-0.19	-0.09 ± 0.22

^aNormal γ -ray energy.

^bSee Ref. 10.

^cSee Ref. 1.

^dSee Ref. 11.

have a delayed component.

Corrections for shifts in the centroid of the unresolved hyperfine multiplets in the $\frac{3}{2}^- - \frac{1}{2}^-$, $\frac{7}{2}^- - \frac{5}{2}^-$, and $\frac{5}{2}^- - \frac{1}{2}^-$ transitions of 30 ± 200 , 40 ± 200 , and 50 ± 200 eV have been calculated.⁹ Our independent estimates of these corrections are in substantial agreement. In the case of the first transition, the half-life of the $\frac{3}{2}^-$ level has been revised from 6 to 0.13 psec. In addition, we have observed and analyzed the γ rays feeding the $\frac{3}{2}^-$ and $\frac{5}{2}^-$ levels.¹⁰ Our analysis enables us to account for the observed intensities of the γ transitions from these levels, and predicts a population distribution between the hyperfine states of each of these levels that is essentially statistical. For the $\frac{3}{2}^- - \frac{1}{2}^-$ transition we find a correction of 10 ± 100 eV.

Our corrected results for the isomer shifts in all three transitions are presented in the final column in Table I (ΔE_{exp}). In column 3 ($\Delta E_{\uparrow, \downarrow}^{\uparrow, \downarrow}$) are listed the shifts for each transition calculated using Eq. (2).

In column 4 (ΔE_F) is one set of predictions for the isomer shifts in ^{207}Pb . The theory of finite Fermi systems was applied to monopole properties in the lead region, including the change in mean square radius between ground and excited states that is partly responsible for the isomer shift.¹¹

In column 5 ($\Delta E_{w.c.}$) is a second set of predictions of the measured isomer shifts. The change in Coulomb binding energy of the muon was analyzed in terms of a single hole coupled to collective vibrations of the nuclear core by means of the weak coupling Hamiltonian. The spread in predicted values results from varying the number of core and single-hole states included in the analysis.

Column 6 (ΔE_E) lists previously quoted experimental results for the three isomer shifts based on unpublished data.¹²

In column 7 (ΔE_{sum}) we have summed the contributions from the anomalous-moment term (col-

umn 3) and the mid-range prediction of the hole-core model (column 5). We note that the agreement with our new experimental results (last column) is improved for the two interdoublet transitions. For completeness we have included the isomer shift in the intradoublet transition.¹³ Here, too, the anomalous-moment term is seen to have an effect in determining the magnitude and possibly the sign of the effect.

We conclude that the spin-orbit interaction of the anomalous magnetic moment of the neutron hole with the electric field of a 1s muon is required to account for the isomer shifts in ^{207}Pb . This term in the muon-nucleon interaction should produce shifts of the order of 0.5 keV in the 1s level of all odd- A heavy muonic atoms.

Comparison of theoretical predictions for the isomer shifts with earlier experimental results suggested the hypothesis that the proton core reacts more significantly to changes in the state of the valence neutron than anticipated by the weak coupling model.² We conclude that this hypothesis is no longer supported by muonic isomer shift data.

It is a pleasure to acknowledge valuable discussions with J. V. Noble, L. Wilets, H. M. Foley, and L. Spruch. We welcome this opportunity to thank R. Siegel, R. Welsh, C. Hansen, and the rest of the SREL personnel for their encouragement and assistance. D. J. Markevich helped with the data analysis. This research was supported in part by the National Science Foundation under Grant No. GP-34527.

^(a)Present address: Varian Associates, Palo Alto, Cal. 94306.

¹R. Bauer *et al.*, Nucl. Phys. **A209**, 535 (1973).

²G. A. Rinker, Jr., Phys. Rev. C **4**, 2150 (1971).

³See S. DeBenedetti, in *Nuclear Interactions* (Wiley, New York, 1964), p. 380.

⁴L. L. Foldy, Phys. Rev. **83**, 688 (1951).

⁵It is worth noting that the Thomas factor of $\frac{1}{2}$ which enters into the spin-orbit interaction for electrons is absent for neutrons.

⁶Of course the neutron experiences the electric field of the 82 protons. However, the resultant electromagnetic spin-orbit splitting is part of the energy of the normal γ (^{207}Pb without a muon), with respect to which we measure our shifts. Such electromagnetic spin-orbit splittings are important in evaluating Coulomb energies of isobaric analog states. See J. A. Nolen, Jr., and J. P. Schiffer, Ann. Rev. Nucl. Sci. **19**, 471 (1969).

⁷W. Bertozzi, J. Friar, J. Heisenberg, and J. W. Negele, Phys. Lett. **41B**, 408 (1972).

⁸D. Kessler, in *Proceedings of the Third International*

Conference on High Energy Physics and Nuclear Structure, edited by S. Devons (Plenum, New York, 1969).

⁹H. Backe *et al.*, Nucl. Phys. **A234**, 469 (1974).

¹⁰B. Budick, R. Anigstein, and J. W. Kast, to be published. A possible resonance due to the near degeneracy of the $4f-3p_{3/2}$ muonic intervals with the $\frac{3}{2}^- - \frac{1}{2}^-$ nuclear interval has been considered. It cannot account for the observed intensity of the nuclear γ ray.

¹¹J. Speth, L. Zamick, and P. Ring, Nucl. Phys. **A232**, 1 (1974).

¹²R. Engfer *et al.*, At. Data Nucl. Data Tables **14**, 509 (1974); see also H. K. Walter, Nucl. Phys. **A234**, 504 (1974), p. 530.

¹³The Foldy term in the matrix element, Eq. (1), contributes only -10 eV to the isomer shift.

Complex Stabilization Method for Resonant Phenomena

B. R. Junker

U. S. Office of Naval Research, Arlington, Virginia 22217

(Received 14 January 1980)

A technique is presented which can be used to compute the complex poles of the resolvent (defined as resonances) directly by use of a square-integrable basis without a coordinate rotation and without explicitly imposing a boundary condition such as a Siegert resonant boundary condition. Such a technique is directly applicable to all phenomena which can be put in the form of a resonance such as photoionization, field ionization, and electron resonances in atoms and molecules.

PACS numbers: 31.15.+q, 34.80.Bm, 34.80.Dp

The description of many interesting phenomena, including field ionization, photoionization (in second quantization), electron resonances in atoms and molecules, and various combinations of these, can be formulated in a resonance picture. That is, the observed structure can be described in terms of the real and imaginary parts (position and width, respectively) of the complex energy, E^{res} , of a pole of the scattering matrix.¹

A number of methods have been developed to try to determine these poles of the S matrix. Prior to the advent of the complex-coordinate method they all required an explicit boundary condition to extract the scattering information. These techniques could be very difficult to apply to phenomena such as field ionization, where the wave function goes asymptotically as an exponential containing fractional powers of the radial coordinate for just the simple case of a hydrogenic system in a constant electric field, and to molecular resonances.

On the other hand, the advantage of the complex-coordinate method² for computing the com-

plex poles of the resolvent operator³ directly is that for a sufficiently large rotation angle, θ , in the transformation

$$r \rightarrow r \exp(i\theta), \quad (1)$$

the resonant wave function $\psi(\theta)$, is square integrable. Thus an explicit boundary condition is not required to extract the complex resonant energy. The direct application of this method to molecules, however, results in complete internuclear separations. Although in principle complex internuclear separations are not a theoretical barrier, the retention of the Born-Oppenheimer approximation with real internuclear separations often offers a desirable picture both conceptually and computationally.⁴

A number of techniques have been suggested recently for applying the complex-coordinate method to molecular systems^{4,5} while attempting to retain the concept of real internuclear separations. These involve external complex scaling or distorted integration contours. I will now present arguments based on previous complex-coor-